Scaling Evapotranspiration Measurements along the Middle Rio Grande Corridor

Middle Rio Grande
Endangered Species Act Collaborative Program

Final Report prepared by Dianne McDonnell, Ph.D. Candidate
and Julie Coonrod, Associate Professor

Contact Information:
Julie Coonrod, Associate Professor
Department of Civil Engineering
MSC01 1070
1 University of New Mexico (505) 277-3233
Albuquerque, NM 87131 jcoonrod@unm.edu

PROJECT DESCRIPTION

Actual evapotranspiration (ET) depletion is one of the most important yet unknown quantities in studies of the middle Rio Grande Basin (USGS 2002). This research uses ground-based measurements and remote sensing techniques to scale evapotranspiration (ET) estimates along the middle Rio Grande riparian corridor in central New Mexico. Previous estimates of riparian evapotranspiration (ET) along the corridor range from between 20 to 50 percent of the total water depletions (Dahm et al. 2002). The University of New Mexico (UNM) Departments of Civil Engineering and Biology have been working to better define ET depletion values in native and non-native flooding and non-flooding field plots within the riparian forest using state-of-the-art micrometeorological techniques. Currently, half hourly ground based micrometeorological data are being collected using the four instrumentation towers installed in cottonwood and saltcedar sites. The tower data form the basis for calculating ET at the four tower sites using the 3-D eddy covariance method (Cleverly *et al.* 2002). These ET values are arguably the most accurate estimates of ET available along the middle Rio Grande corridor. However, they are limited to only four points along the 320-kilometer riverine corridor. This research better defines total ET depletions by calibrating remote sensing imagery with these plot scale measurements of ET. Better spatial and temporal estimates of ET provide important information for static models. In addition, the resulting spatial and temporal distribution of ET provides insight on the role of ET along the corridor as a function of location, time of year, and as a comparison between a drought year and a relatively wet year.

There are three elements required to scale ET to the corridor.

I. **Classifying habitat along the middle Rio Grande riparian corridor using Landsat 7 ETM+ imagery.** This section describes the distribution of habitats as they relate to Potential ET depletions.

II. **Estimating evapotranspiration depletions in *Tamarix* and *Populus deltoides* canopies at the plot scale along the along middle Rio Grande riparian corridor.** This section solidifies the idea that vegetation density can be used to scale ET to the riparian corridor.

III. **Scaling ET to the entire middle Rio Grande Corridor using Landsat 7 ETM+ imagery.** Based on the culmination of elements I and II,

I. Classifying vegetation along the middle Rio Grande riparian corridor using Landsat 7 ETM+ imagery.

1. Introduction

The middle Rio Grande riparian corridor extends about 320 kilometers from the Otowi Bridge to Elephant Butte stream gages (Dahm *et al.* 2002). Figure I-1 shows the middle Rio Grande watershed in central New Mexico and identifies the four reaches defined by the Bosque Biological Management Plan. Characterizing the temporal distribution of riparian habitat is the first part of an on-going research project to scale evapotranspiration (ET) depletions along the middle Rio Grande riparian corridor in central New Mexico. Toward that initial goal, this paper presents a technique for creating dynamic three-dimensional (3D) habitat maps using Landsat 7 ETM+ imagery and the decision tree classifier in ENVI 4.0. The resulting maps can be produced with sequential cloud-free images to illustrate the temporal shifts in agriculture, grasslands, wetlands, and forested canopies. In addition, these maps can be compared to historic maps to assess the changes along the middle Rio Grande. A comparison is made between a June 2001 map produced in this study and a 1935 classification map provided by the Army Corps of Engineers (COE) and previously published in the Bosque Biological Management Plan (BBMP) (Crawford *et al*. 1993). The historic comparison looks at the changes in native and non-native habitats along the riparian corridor. A seasonal comparison is made between the June image and a May, 2002 image to illustrate the changes in habitat in different months.

2. Site Description

Historically the middle Rio Grande floodplain was a braided, slightly sinuous river that broadly meandered laterally within the 2-km to 6-km wide floodplain. The native forests or "Bosque" were dominated by cottonwood (*Populus deltoides* ssp. *Wislizeni),* and willow (*salix* sp) of varying ages, sizes, and configurations (Molles *et al*. 1998 and Crawford *et al.* 1993). The Bosque was interspersed with open areas of grass meadows, ponds, small lakes, and marshes. The dynamic effects of flooding perpetuated a changing mosaic of the river's historic landscapes (Crawford *et al.* 1993). The first evidence of decline occurred between 1880 and 1896 (NRC 1938). The decline was attributed to an increase in seeped and waterlogged areas caused by a decrease in flow in the river. By the 1920s, the newly formed Middle Rio Grande Conservancy District (MRGCD) approved and implemented a plan for flood control, drainage, and irrigation (NRC 1938 and Crawford *et al.* 1993). The construction of dams, levees, and Kellner jetty jacks in the mid 1930s channelized the river and played a major role in defining the existing riverine corridor. Drainage resulted in the dramatic disappearance of lake and marsh communities. Wetland vegetation migrated to ditches and drains (Crawford *et al.* 1993). Flow regulation practices have resulted in an invasion of exotics including Russian olive (*Elaeagnus angustifolia*), saltcedar (*Tamarix chenesis*), and Siberian elm (*Ulmus pumila*) (Crawford *et al.* 1993). All three exotic species are found intermixed and in the understories of native cottonwood stands. Saltcedar also can be found in dense monotypic stands in both flooding and nonflooding areas. The maps produced in this research identify the broad categories of native and non-native habitat in today's highly regulated Rio Grande.

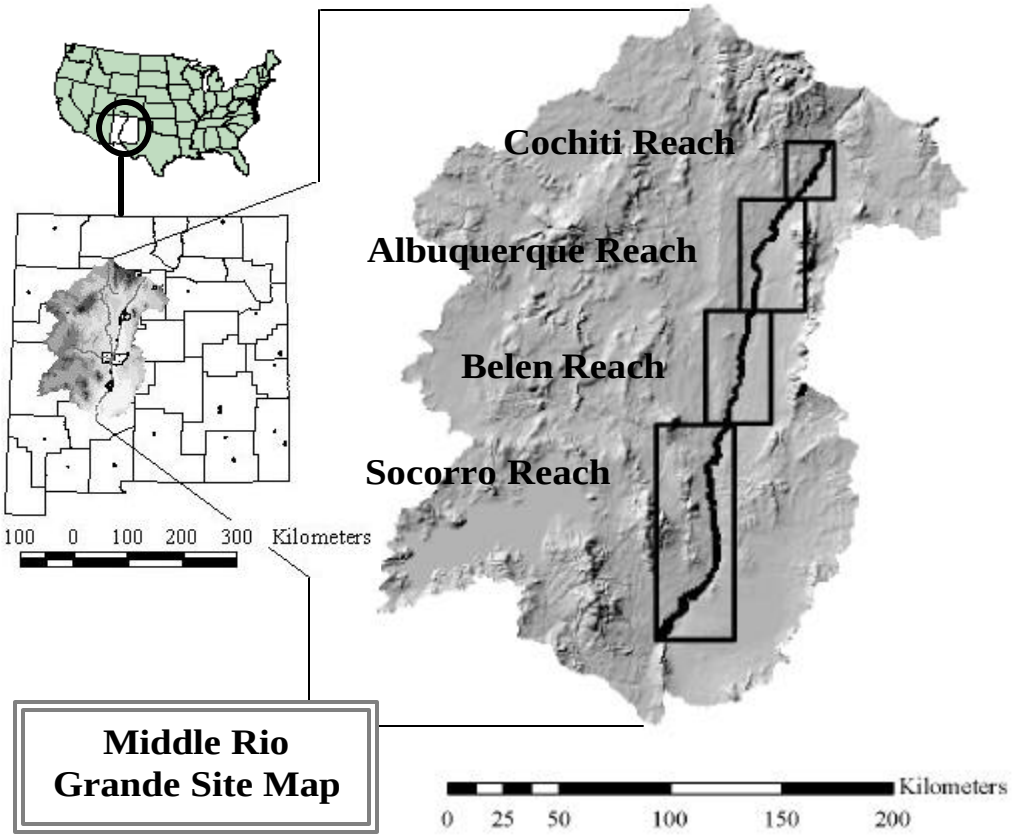

Figure I-1. The middle Rio Grande in central New Mexico. For this study, the region is divided into four reaches which start immediately below the Cochiti reservoir and end above the Elephant Butte Reservoir. Each reach is separated by a USGS stream gage.

3. Methodology

The ability of Landsat imagery to distinguish water and vegetation based on spectral properties is well documented. Table 1 lists the eight bands measured by Landsat 7 ETM+ and describes specific uses for each band. Several reports show that red, near infrared (NIR) and mid infrared (MIR) bands are useful in detecting chlorophyll, vegetation, soil moisture, water, and leaf structure. The technique developed in this research uses these bands and the decision tree classifier in ENVI 4.0 to create dynamic 3D habitat maps. Although, the procedure is presented in a step-by-step format, the actual process is iterative. It requires tweaking of the rules to clarify the blurred boundaries between habitat classes in order to create 2D habitat classification maps. Overlaying 2D maps onto relief maps based on an index related to potential ET produces 3D classification maps. These maps define the boundaries between classes with greater detail than the 2D maps.

3.1. Decision Tree Classifier

The decision tree classifier in ENVI is new to version 4.0. An earlier version of this same classification technique is done without the benefit of the decision tree classifier. (McDonnell *et al*. 2003). The classifier simplifies the process of applying a hierarchal series of rules to the region in order to differentiate habitats. Specifically, the classifier performs

multistage classifications based on “yes” or “no” answers to expressions or rules (ENVI users manual 2004). The expressions used in the classifier may come from any source with the same geographic positioning. Examples of sources include masks defined by polygons or shapefiles, images captured by different sensors, or images taken on different dates. Each decision divides the pixels within an image into two classes. The pixels in each new class can be divided into two more classes based on the next expression. The resulting tree can be as simple as two classes or infinitely complicated.

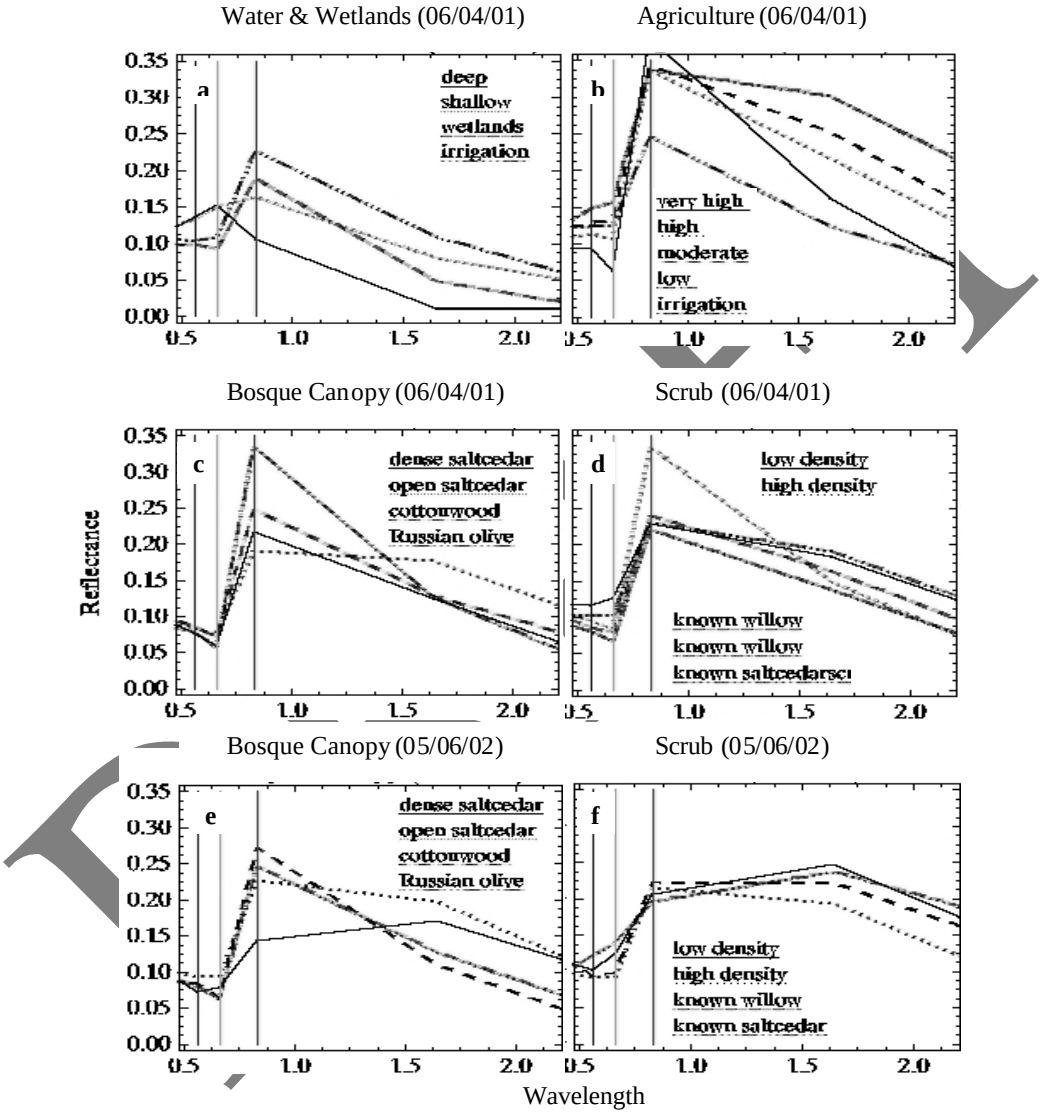

Figure I-2. Spectral signatures for representative habitats. High reflectance in the red and low reflectance in the NIR and MIR represent wet areas. High absorption in the red with high NIR reflection indicates green vegetation. The higher absorption in the MIR bands represents higher water content in the leaves.

This technique takes full advantage of the decision tree classifier’s ability to incorporate multiple images. Two images are used to distinguish habitat. These images represent a shift in

the way habitats behave at different times during the growing season. The patterns in spectral signatures of the June 4, 2001 image enable us to distinguish vegetation and water. Water tends to reflect red and absorb NIR and MIR light (Figure I-2a). The June 2001 image is particularly useful in capturing water because it occurs shortly after a planned flood release from the Cochiti reservoir. Figure I-2c and d shows that vegetation tends to reflect NIR and absorb red. Although, the June image can distinguish vegetation and water, it cannot distinguish between vegetation.

The patterns in the May 6, 2002 image help to further differentiate vegetated habitats. We believe this is because the May 6, 2002 image represents a period of stress. Night time temperatures are low and drought conditions persist in May 2002. We know that physiological processes of plants differ in their response to seasonal stresses (Lambers *et al*. 2000). For example Aspen (*Populus tremuloides*) leaves develop on short shoots that go through winter with preformed buds (Archibold & Ripley 2004). Their leaves emerge quickly at the start of the growing season. Similarly, Figure I-2e and f show that in 2002 cottonwood and Russian olive canopy exhibit spectral properties indicative of early leaf-out and transpiration compared to the more shrub-like saltcedar and willow canopies. In particular, the May signatures (Figure I-2e and f) show high reflectance in the MIR bands for saltcedar and willow. Cottonwood and Russian olive habitat tend to have higher NIR and lower reflectance in the MIR bands in the May image. In both the June and May images, the main points of interest within the signatures lay in the red, NIR, and MIR wavelengths.

Normalizing NIR and red reflectance yields the normalized difference vegetation index (NDVI). Gamon *et al.* (2004) analyze the relationship between NDVI, canopy structure, and photosynthesis in Californian canopies. That study shows good correlations with sparse canopies but when leaf area index (LAI) exceeds 2, sensitivity decreases. Red light is absorbed by chlorophyll within the first layer (LillesETer 1982, Goa 1996, and Anderson *et al*. 2004). When LAI levels are greater than 3, NDVI is saturated (Goa 1996). Bosque habitats typically have LAI measurements between 2 and 5; therefore, NDVI has limited application in these forested habitats.

NIR and MIR wavelengths are known to penetrate through eight leaf layers (Goa 1996). Using Landsat imagery, Frazier and Page (2000) achieve success in locating water using NIR and MIR bands. An AVIRIS index, known as the normalized difference wetness index (NDWI), identifies liquid water in vegetation (Goa 1996 and Gao & Goetz 1995). NDWI has also been defined using SPOT and Landsat 7 imagery. NDWI measured with SPOT imagery is suitable for estimating the water per unit area of vegetation (Maki *et al*. 2004). A Landsat NDWI, using bands 4 and 5, is more sensitive than NDVI to leaf area and water content in closed canopies and saturates at higher LAI values (Anderson *et al*. 2004). Expressions based on NIR, NDVI, and Landsat wetness indices are applied to the May and June images to develop 2D classification maps.

The Landsat indices used in this research are defined as follows:

NDVI = [NIR (0.84 µm) – MIR (0.66 µm)] / [NIR (0.84 µm) + MIR (0.66 µm)]
PETI[1] *= [NIR (0.84 µm) – MIR (1.65 µm)] / [NIR (0.84 µm) + MIR (1.65 µm)]*
NDWI-2[2] *= [NIR (0.84 µm) – MIR (2.21 µm)] / [NIR (0.84 µm) + MIR (2.21 µm)]*

1. PETI = *Potential ET Index (highly correlated to ET in a parallel study). PETI is also called NDWI in other studies but because all NIR and MIR normalizations are labelled as NDWI, we chose to differentiate PETI from the other NDWI numbers.*
2. NDWI-2 = Does not correlate to ET but has been used as a wetness index in Anderson *et al*. (2004).

3.2. Adding Relief to the Classification Maps

Adding spectral and textural characteristics to improve classification accuracy has been tried in a number of studies (Innes and Koch 1998). In one study, texture improves class segmentation (Ryherd and Woodcock 1996). In another study, a principle components analysis of red, NIR, and MIR helps, to some extent, distinguish boundaries between classes (Abeyta and Franklyn 1998). In this study we create a relief map of PETI to help define the fuzzy boundaries between habitats and characterize the roles different habitats play within the ecosystem. The PETI relief map is created in ENVI 4.0 for June, 2001 and May, 2002. An overlay of the classification for that particular month is placed on the PETI relief map. We set classification transparency at 40% to allow texture to show through the classification maps. The texture distinguishes areas with high PET. Inorganic dry areas will have low PETI values and therefore look flat while heavily transpiring vegetation will have a raised appearance that we believe relates to the level of water consumption.

3.3. Calibration and verification

Calibration is primarily based on 16 sites and 110 points along the middle Rio Grande. Photos of one point in the 12 calibration sites are shown in Figure I-3. These main calibration sites are also research sites instrumented to measure a variety of biotic and abiotic parameters. Figure I-4 shows a typical configuration of the calibration sites. The wells at each site have GPS coordinates to help locate habitat types in the georeferenced images. The photos illustrate the heterogeneous nature of many of the sites and the difficulties that arise in developing an ontology that would allow us to compare these maps to other maps. These points and points at the other four calibration sites help establish the expressions or rules used in the classifier. Areas readily apparent in the images, like sand and water, do not require GPS calibration points. In addition, it is assumed that wetlands and irrigated agriculture have a strong water signal and a moderate NDVI or green signal. Once the maps are complete, field verification at bridges and near the original calibration points are used to improve accuracy.

4. Results

The decision tree, shown in Figure I-5, successfully differentiates broad categories of habitats. Most of the expressions shown in the decision tree can be used with any image. There are however, some rules that require an index from a specific month. Expressions that contain M or J with the index indicate that either the May or June index is required in that particular rule. For example, MPETI refers to May PETI and must be used to separate shrub-like vegetation from tree-like vegetation. The decision tree in Figure 5 can be applied to any image in 2001 and 2002. Executing the decision tree classifier using the rules in Figure I-5 produces a 2D classification map. Overlaying the 2D classification map on the PETI hillshade enhances the detail. The resulting maps are informative 3D classification maps. The northern and southern reaches are shown in Figures I- 7 and I-8 respectively.

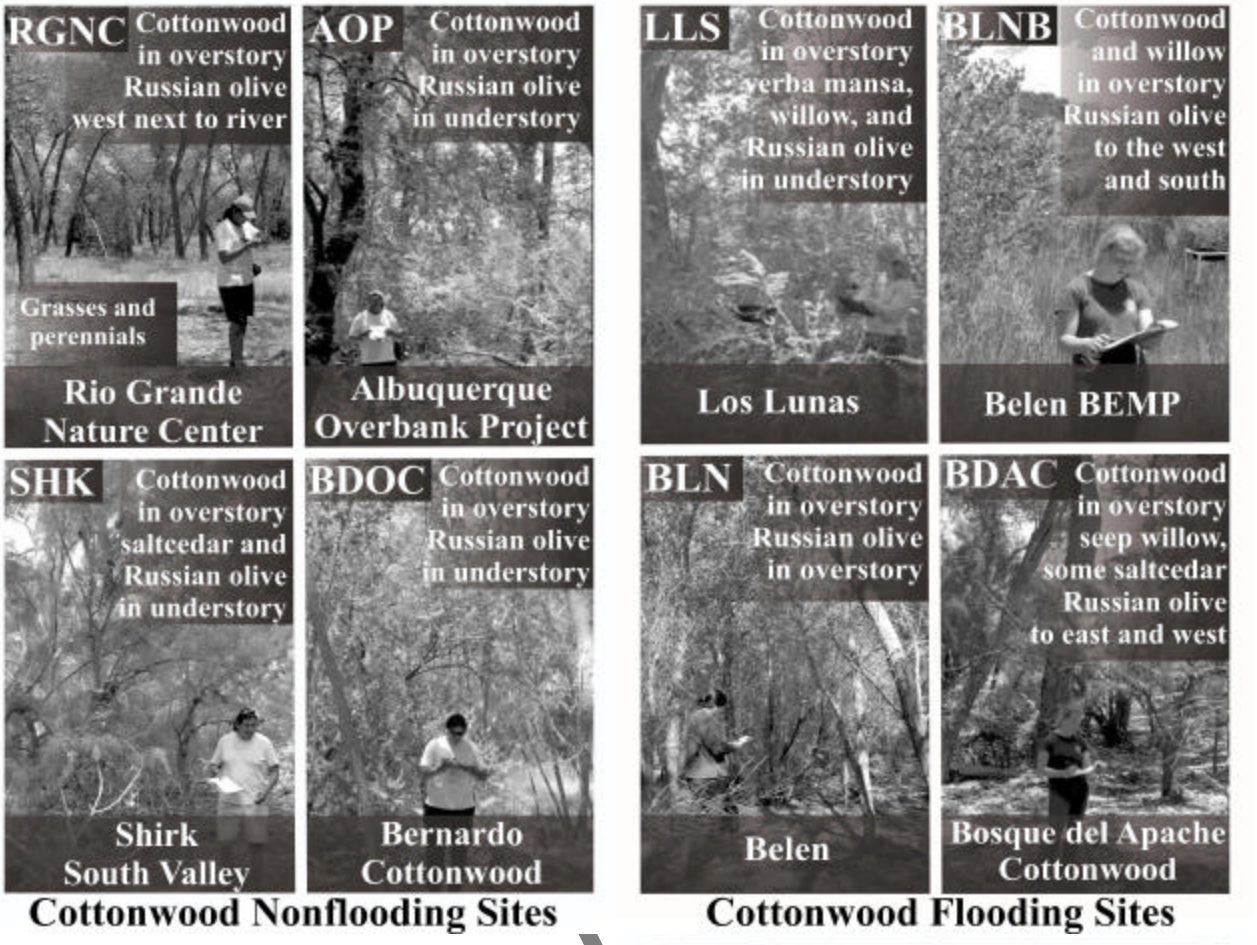

Figure I-3 – Photos of 12 calibration sites. The photos are grouped first by canopy type and second by the flooding regime.

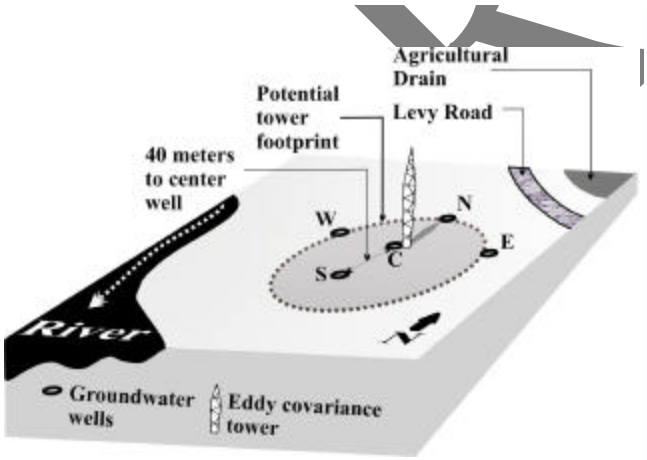

Figure I-4 – Typical layout of the calibration sites. Four wells are located 40 meters in each cardinal direction from a center well. Four of the 12 study sites have instrumentation towers. The tower is located near the center well.

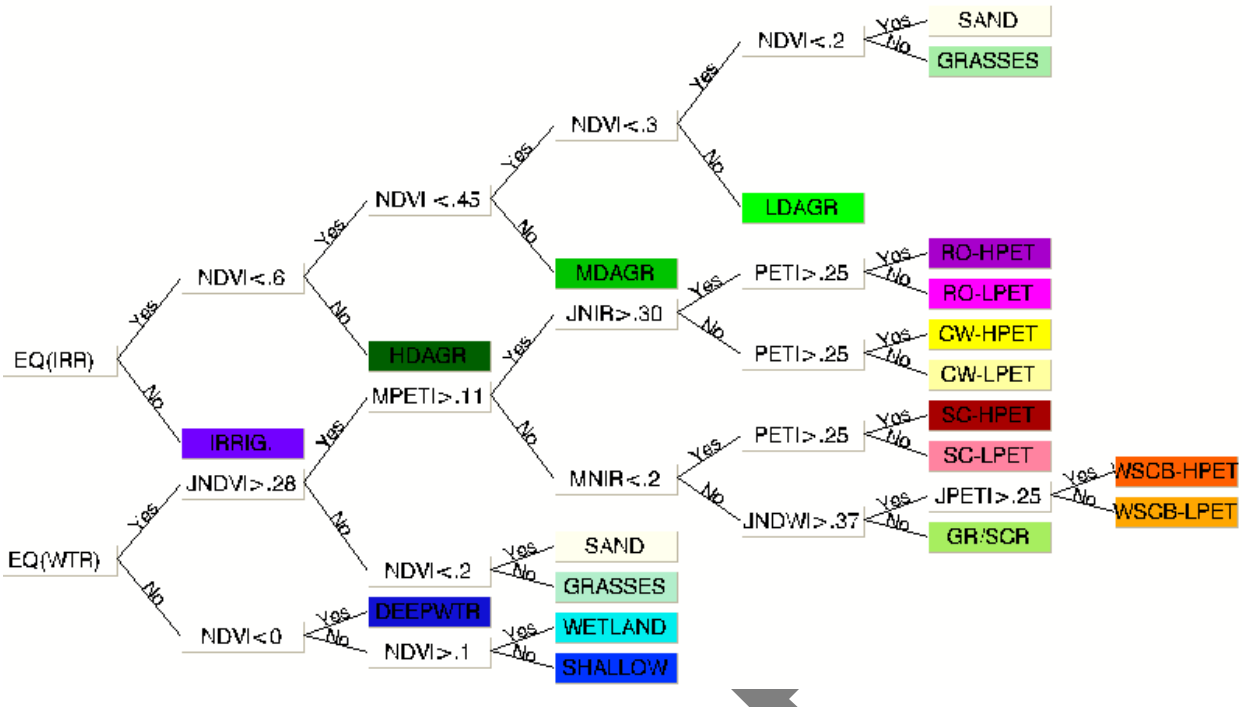

Figure I-5: Bosque decision tree constructed in ENVI 4.0. The expressions are applied to each remaining set of pixels in a hierarchal system. If a month is indicated then that month is used for all images. *J = June 4, 2001 and M = May 6, 2002.*

EQ(IRR): (NDVI + 0.135) > NDWI-2 OR NDWI-2 < 0.3 ***EQ(WTR): (NDVI + 0.135) > NDWI-2***

5. Discussion

The benefit of these maps lay in their ability to represent the riverine corridor's temporal and spatial dynamics. Although the dataset is limited, the temporal and spatial distribution of ET in these maps contradicts conventional wisdom. Native and non-native habitats are believed to consume 20 - 50% of total water budget along the river (Dahm *et al*. 2002). Exotic species are blamed for increases in ET depletions (Robinson 1958, Sala *et al.* 1996, Cleverly *et al*. 1997, & Dahm *et al*. 2002). Tickner *et al*., (2001) recommends eliminating saltcedar from riparian areas to reduce water consumption. In these maps, cottonwood and Russian olive habitat appear to consume more water than saltcedar and willow habitat. This may or may not be true over the entire growing season. There may be specific abiotic factors associated with this apparent anomaly. A complete analysis requires multiple images over a growing season and perhaps over several years to see consistent patterns in the various habitats.

6. Progress

This work is complete.

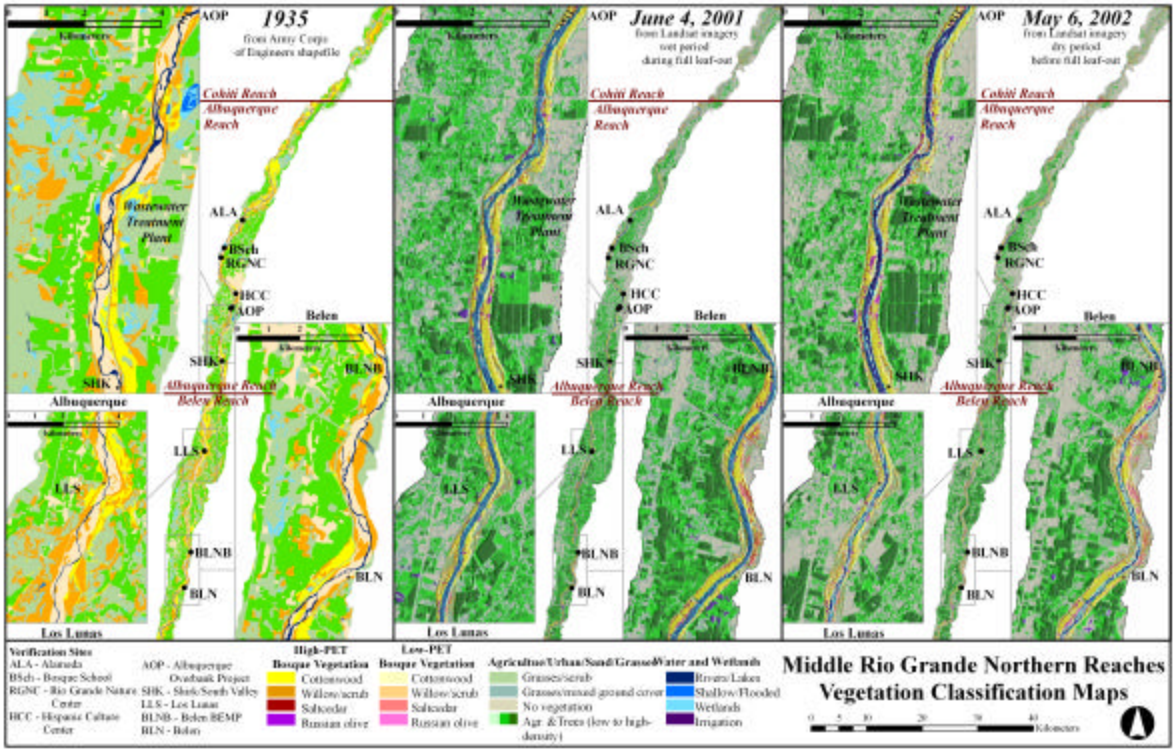

Figure I-6. Middle Rio Grande Habitat Classification Maps (Northern Reaches)

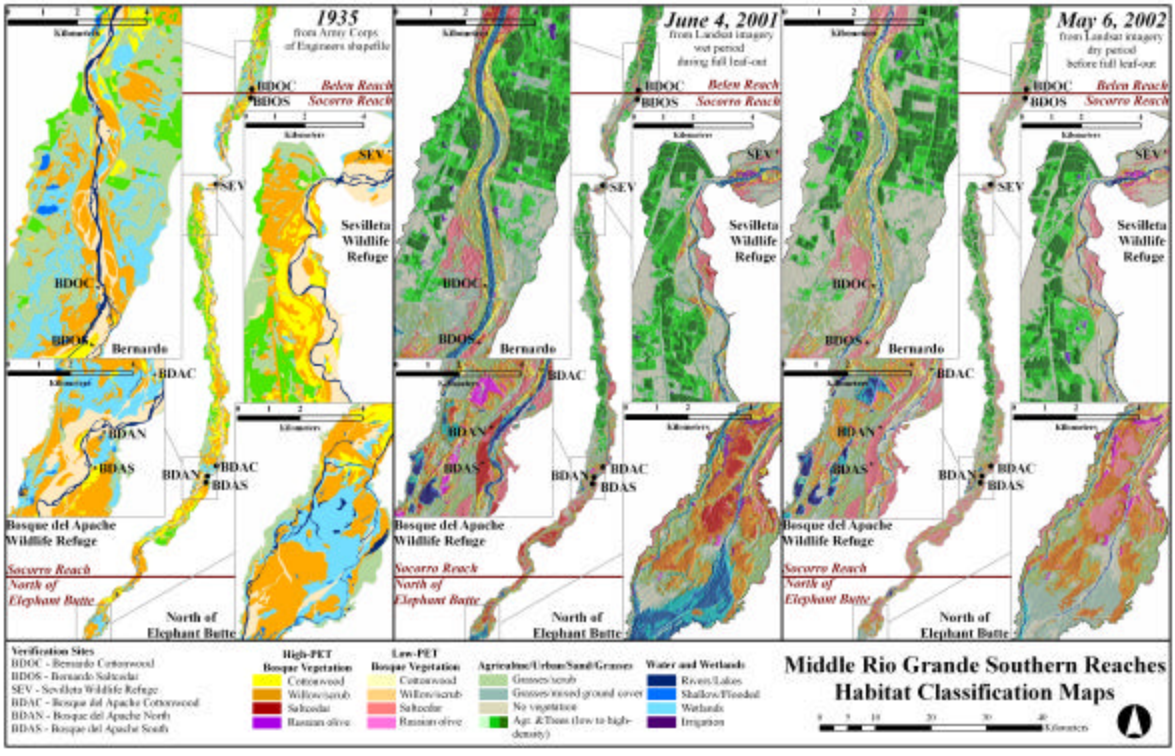

Figure I-7. Middle Rio Grande Habitat Classification Maps (Southern Reaches)

II. Estimating Evapotranspiration Depletions at the plot scale in *Tamarix* and *Populus deltoides* Canopies along the along Middle Rio Grande Riparian Corridor in Central New Mexico

1. Introduction

Traditional methods use micrometeorological data to scale ET. Because we are interested in the role vegetation plays in ET depletions, this work focuses on using a vegetation index to scale ET. The goal of this research component is to determine if leaf area index (LAI) measured using a LICOR 2000 LAI meter can be used to scale actual evapotranspiration (ET) depletions from four sites with 3D eddy covariance towers to multiple plots along the middle Rio Grande riparian corridor in central New Mexico.

2. Site Description

The University of New Mexico is working to quantify the effects of native versus non-native canopy on ET depletions at 12 study sites along the middle Rio Grande riparian corridor. Instrumentation towers are installed at four representative ecosystems including a nonflooding cottonwood site, a flooding cottonwood site, a nonflooding saltcedar site, and a flooding saltcedar site (Figure II-1). The towers provide half hourly integrated measurements of ET. These sites form the basis for calibrating ET at eight other representative sites within the region. Figure II-1 shows the location of all 12 study sites. The layout of a typical study site with an eddy covariance tower is shown in Figure II-2. All 12 study sites have groundwater wells installed to monitor water table fluctuations. The wells are oriented with a center well and four additional wells positioned approximately 40 meters in each cardinal direction. It should be noted that this work was initiated prior to installation of the La Joya tower; thus the La Joya tower is not included. The Belen tower was vandalized during the summer of 2004 and is no longer in operation.

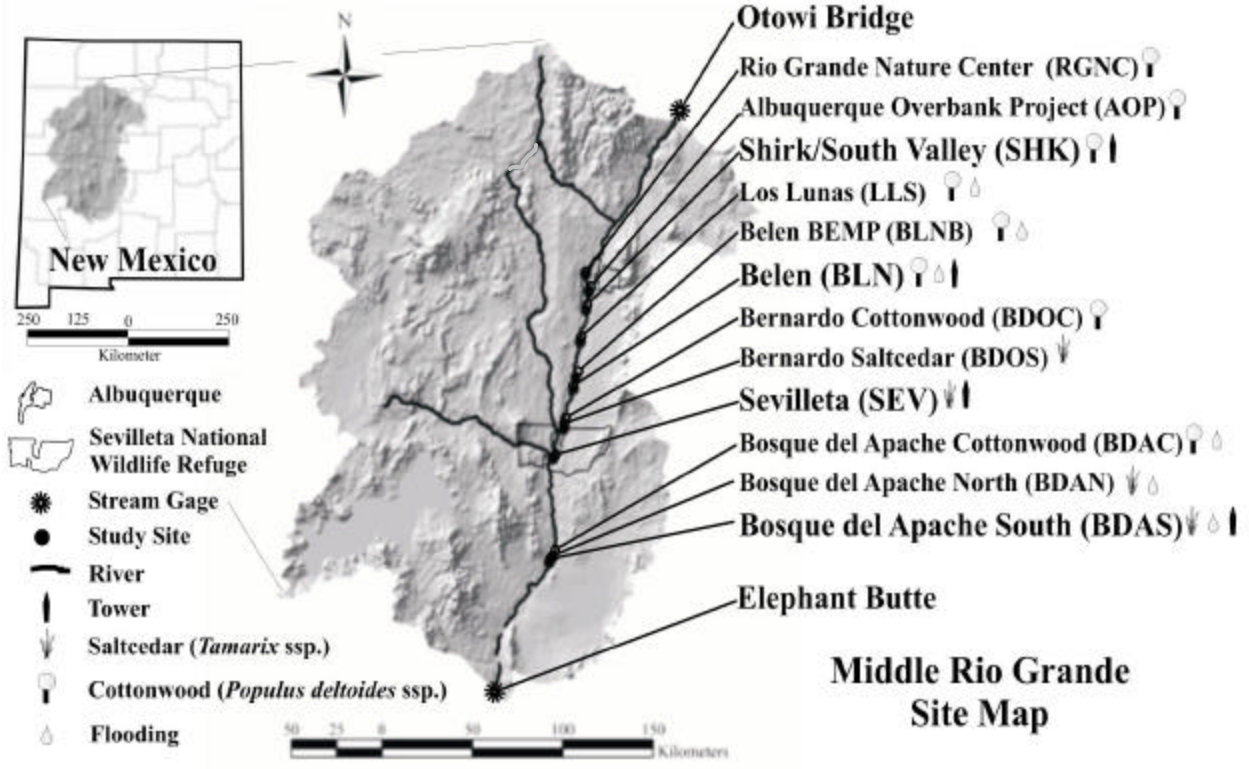

Figure II-1. Middle Rio Grande with study sites identified.

3. ET at the Tower Sites

The 3D eddy covariance towers have been instrumented to quantify the various parameters in the energy balance equation. Figure 3a is an example of an instrumented tower at the Sevilleta saltcedar nonflooding site. The energy balance equation is based on the conservation of energy where energy inputs equal energy outputs. Figure 3b illustrates the daytime flow of energy in and out of a forested surface. Net radiation (Rn) is the term used to describe the flow of energy into the canopy. Rn is the percent of short-wave radiation not affected by albedo minus long-wave radiation. During the day, this value is positive since solar radiation exceeds long-wave radiation. At night Rn is negative. All other energy terms must sum up to equal Rn as shown in equation 1.

Figure II-2. Typical study site configuration. This image has a tower located at the center well.

equation 1: $Rn = LE + H + G + S + Advection$

Rn = net radiation, LE = turbulent latent heat flux to the atmosphere (E = evaporation, L = latent heat of vaporization), H = turbulent sensible heat flux to the atmosphere, G = ground heat flux, S = canopy heat flux, and Advection = lateral transport of energy (Barry & Chorely 1998).

Ground heat flux (G), latent heat flux (LE), and sensible heat flux (H) are readily measured at the tower sites. Soil heat flux plates measure the heat conducted from the ground surface into the soil (G). Eddy covariance is used to calculate LE and H. Eddies are parcels of air that transport energy, momentum, and moisture from the forested canopy to the atmospheric boundary layer just above the canopy (Barry & Chorely 1998). Instruments (Campbell Scientific) are affixed to the towers, positioned approximately 1.5-2 meters above the canopy (Dahm *et al.* 2002). The instruments on the towers measure vapor and heat fluxes. These fluxes are

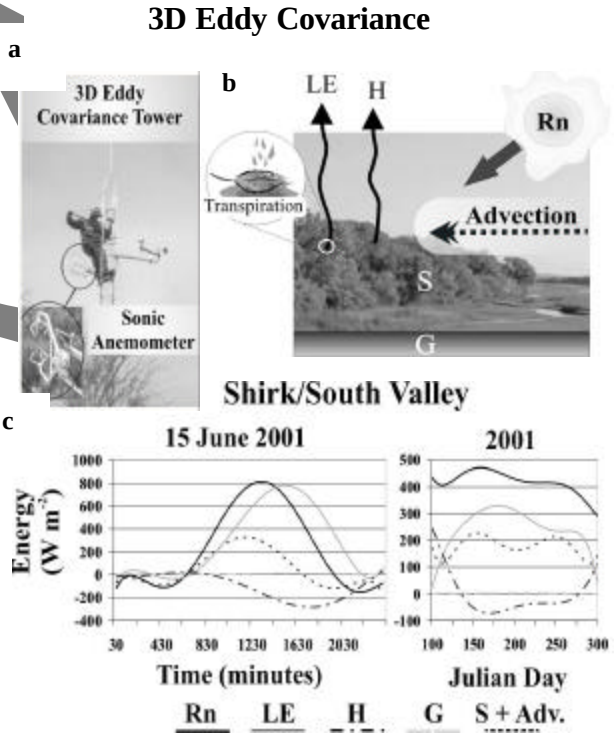

Figure II-3. The energy budget as it applies to the riparian canopy. a) Instrumentation tower at Sevilleta. b) Daytime energy transport in and out of the canopy. c) Daily and seasonal energy budget at Shirk/south valley.

statistically correlated with vertical wind velocities to determine the net transport of LE and H (Dahm *et al.* 2002). A three dimensional sonic anemometer measures vertical wind velocities. It also measures virtual temperature as a function of pressure, specific heat, gas constant for air, and the speed of sound. Virtual temperature is corrected for specific humidity. A krypton hygrometer measures vapor pressure.

Canopy storage (S) + Advection cannot be measured directly. S is a relatively small term. Unfortunately advection, the lateral transport of energy by wind, can be quite large. S + Advection are determined by solving the energy balance equation. A percent of this value is reallocated to LE using the Bowen Ratio (equation 2). Total LE is then calculated (equation 3). Finally ET can be determined (equation 4).

equation 2: LE = H/(S + Advection) => if H is < 0 then LE = (S + Advection)
equation 3: LE(total) = LE(eddy covariance) + LE(Bowen ratio)
equation 4: ET = LE(total) / $\lambda_v \rho_w$

ET=actual evapotranspiration, λ_v = latent heat of vaporization, and ρ_w = density of water.

Half hourly values for Rn, LE, H, G, and (S + advection) are quantified. Figure 3c shows the change in these fluxes at the Shirk/south valley site over a 24 hour period for June 15, 2001 and over the growing season.

4. Methodology

4.1. Overview

Seasonal ET depletions in forested areas are controlled by multiple factors including leaf surface area, the length of day, the leaf temperature, the tree species and its age, and climate (Barry & Chorely 1998). With the exception of tree age, the factors described by Barry & Chorely (1998) are used to determine ET within the forested canopies along the middle Rio Grande riparian corridor. Using multiple regression analysis, a measure of leaf surface area, percent daylight, and a correction for temperature are calibrated with ET calculations at the 3D eddy covariance towers in four representative ecosystems.

4.2. Leaf Surface Area

Sala *et al.* (1996), and Cleverly *et al.* (1997) both show, on a leaf area basis in a Mojave desert floodplain, that *Tamarix* ssp. do not consume more than the native species. There have long been assertions that the invasive *Tamarix* ssp. consumes more water than native species (Davenport *et al.* 1982 and Tickner *et al.* 2000). In order for a *Tamarix* ssp. canopy to consume more water, it would need to form a denser stand than its native counterpart. We test two techniques for

Figure II-4. LICOR LAI-2000 meter used to measure LAI at the 12 study sites

measuring leaf surface area. One technique is a field based measurement of leaf area index and the other is based on a potential ET index (PETI) derived from Landsat 7 imagery.

Field measurements of LAI were taken at each of the five wells (Figure II-2) of the 12 study sites using a LICOR LAI-2000 meter during the 2001 and 2002 growing seasons. Figure II-4 shows a field investigator measuring LAI at the Sevilleta saltcedar site. The LAI-2000 calculates LAI based on blue reflectance measurements made with a "fish-eye" optical sensor (148° field-of-view) (Wells and Norman, 1991). Above-canopy and below-canopy measurements were taken. The above canopy shots were used to subtract the sky from the leaf area. Multiple below-canopy readings and the fish-eye field-of-view insure that LAI calculations were based on a large sample of the foliage canopy. The control unit performed all calculations. All measurements were taken at dusk or under cloud cover because measurements taken in bright sunlight would tend to underestimate leaf area (Wells and Norman, 1991). Figure II-2 illustrates a footprint associated with the tower sites. These footprints vary in size and direction depending on wind speed and direction. The cartoon in Figure II-2 shows the footprint favoring the southern part of the site because prevailing winds are often from the south. Although it is impossible to match the footprint completely, the average LAI values at all five wells provide a good representation of LAI for each tower site.

4.3. ET increases with day length independent of vegetation type.

Day length is significant since transpiration is linked to photosynthesis. Leaves and their stomata, specifically their guard cells, respond to light. The stomata will only open when CO_2 can be assimilated thus preventing unnecessary water loss (Lamberts *et al.* 1998).

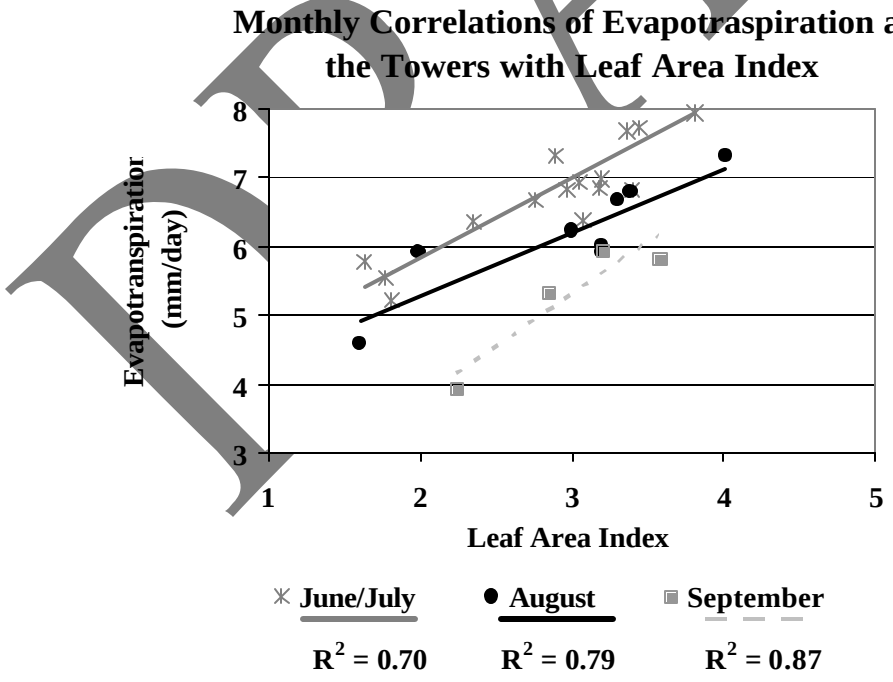

4.4. ET is suppressed at high and low temperature extremes

Temperature affects all biochemical reactions of photosynthesis and subsequent responses to temperature are complex (Taiz and Zeigler 1998). Plants generally have optimum temperatures for photosynthesis that reflects the combined effects on both gross photosynthesis and respiration (Taiz and Zeigler 1998; Aber and Mellilo 2001). CO_2 assimilation is suppressed at low temperatures and high temperatures (Taiz and Zeigler 1998). A correction for high and low temperature extremes is applied to the estimate ET values.

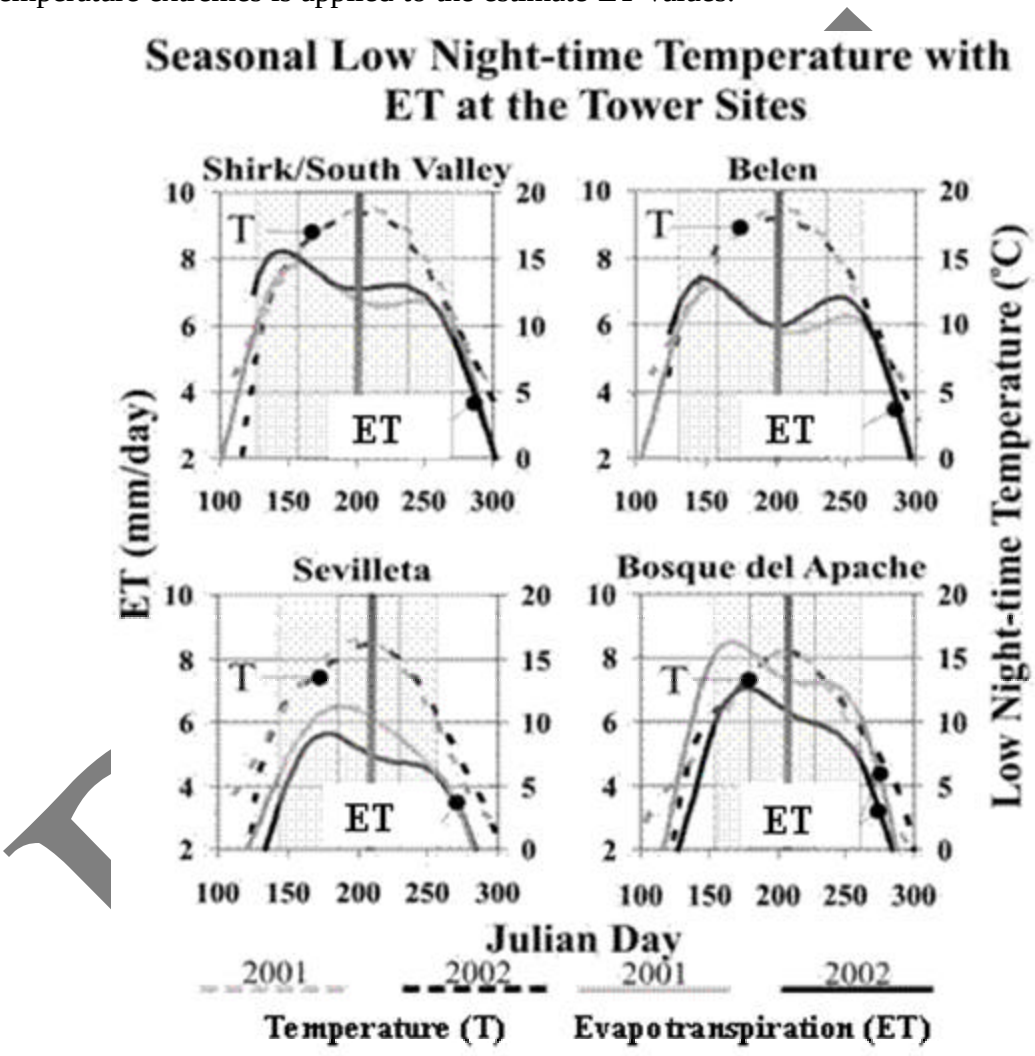

Figure II-5 – Daily low night-time temperature plotted against ET depletions

5. Results

5.1. Multiple regression analysis

The results of the multiple regression analysis are presented in figure II-5. The results show a high correlation between LAI with temperature and daylight corrections and ET.

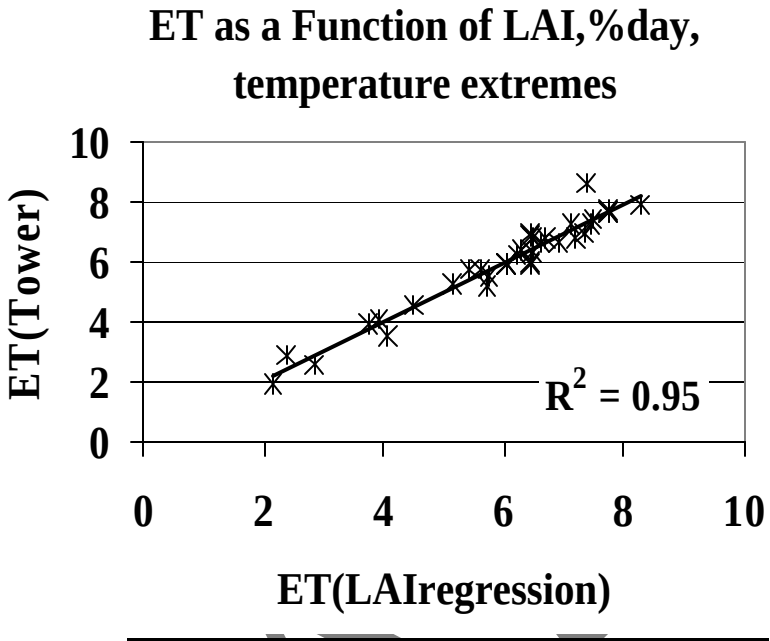

	Standard Error	t Stat	P-value
LAI	0.10	12.39	<0.01
%Day	1.64	10.80	<0.01
Tcor	0.14	-14.14	<0.01
Intercept	0.98	-7.21	<0.01

Figure II-6. Multiple regression of ET as a function of LAI, day length, and high and low temperature extremes. ET(Tower) is the ET calculated with the 3D eddy covariance towers.

5.2. Seasonal accumulation of ET at the 12 study sites.

Figure II-7 shows the seasonal accumulation of ET at the 12 study sites.

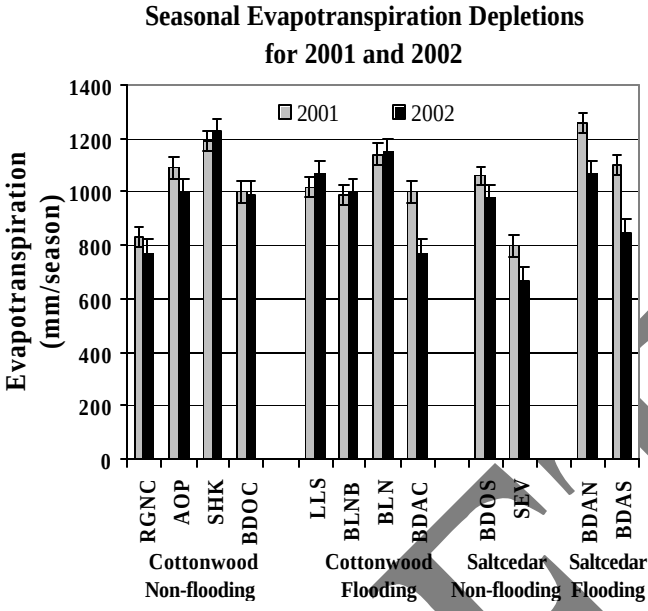

(a) Cottonwood Non-flooding Sites (mm/season)

	RGNC	AOP	Shirk	BDOC
2001	830	1090	1190	1000
2002	770	1000	1230	990
Change	-60	-90	40	-10

(b) Cottonwood Flooding Sites (mm/season)

	LLS	BLNB	BLN	BDAC
2001	1020	990	1140	910
2002	1070	1000	1150	770
Change	50	10	10	-140

(c) Saltcedar Sites (mm/season)

	BDOS	SEV	BDAN	BDAS
2001	1060	800	1260	1100
2002	980	670	1070	850
Change	-80	-130	-190	-250

Figure II-7. Seasonal ET depletions at each study site calculated using an equation developed with a multiple regression analysis. The regression is based on LAI, temperature extremes, and day length.

6. Progress

The analysis of this work is complete.

III. Scaling ET to the middle Rio Grande Riparian Corridor in Central New Mexico for 2001 and 2002

1. Introduction

This research element is the culmination of research elements I and II. Research element I found an apparent link between ET and a vegetation index using remote sensing imagery. Research element II found a link between vegetation and ET using a ground based LAI meter. The question regarding the total consumption of ET along the middle Rio Grande riparian corridor by native and non-native canopy types cannot be answered by looking at a single map of ET. These maps are only snapshots of ET depletions. Calculating ET for the entire growing season better defines the total depletions between native and nonnative canopies. Because measurements were taken during a relatively wet year (2001) and a drought year (2002), we can also compare how different vegetation types behave in different climatic conditions.

2. Methodology

Based on the results of step one, LAI and ET are nearly interchangeable in this ecosystem. Therefore, if Landsat 7 can be used to determine a similar vegetation index, then it can be used to determine ET. Turner *et al.* 1999 and Schultz and Engman 2000 provide two distinct equations relating LAI with Landsat 7 imagery using NDVI. We know from chapter one that NDVI is saturated within the first leaf layer. Rather than using NDVI, we use PETI from chapter I. The comparison between ET and PETI is made with the average values of all five points. The indices are based on the reflectance properties measured by Landsat 7. The accuracy of the imagery is approximately +/- 15 meters. This means the measurement points may not be in the actual grid cell. The larger footprint minimizes the errors associated with rectifying the imagery and with the inaccuracies of GPS.

3. Results

3.1. Multiple regression analysis

The results of the multiple regression analysis shows a high correlation between PETI with temperature and daylight corrections and ET.

3.2. Applying the resulting equations to Landsat imagery

Figure III-1 illustrates the application of the resulting equation on remote sensing imagery.

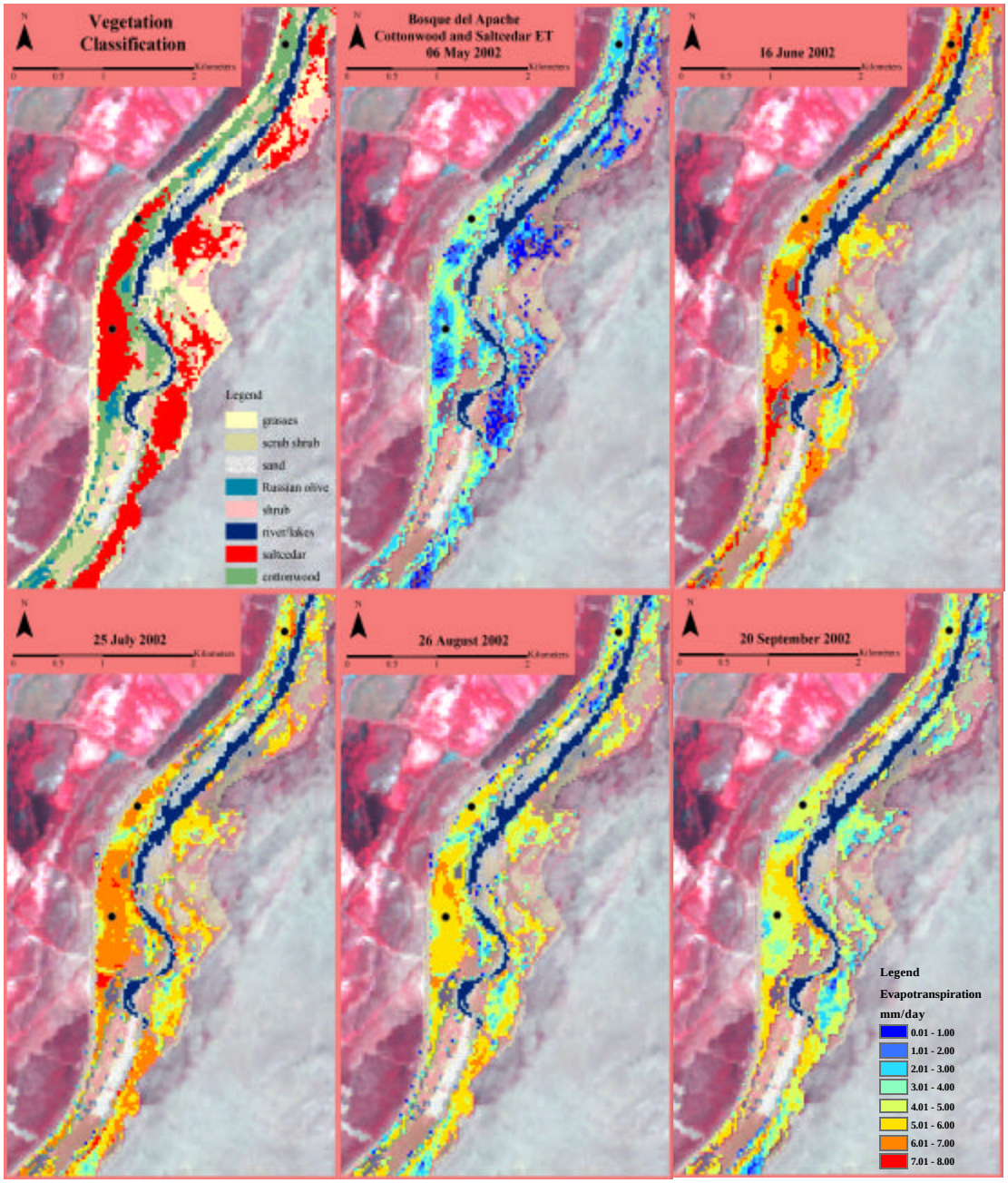

Figure III-1. Monthly ET depletions at Bosque del Apache calculated using an equation developed with a multiple regression analysis. The regression is based on PETI, temperature extremes, and day length.

4. Progress

The basic analysis is complete. The following tasks still remain.

- Process remaining images
- Apply the equation to all images
- Fit a 6^{th} order polynomial through each pixel, integrate the area under the resulting curve and calculate the seasonal ET maps.

REFERENCES

Anderson, M.C., Neale, C.M.U., Li, F., Norman, J.M., Kustas, W.P., Jayanthi, H., & Chavez, J. (2004). Upscaling ground observations of vegetation water content, canopy height, and leaf area index during SMEX02 using aircraft and Landsat imagery. *Remote Sensing of Environment*, 92, 447-464

Anthes, R.A., (1992). *Meteorolgoy 6th edition*. (pp. 106). New York: Macmillan Publishing Company

Barry, R.G., & Chorley, R.J. (1998). *Atmosphere, weather and climate 7th edition*. (pp. 111-112). New York: Routledge

Chandrasekaran, B., Josephson, J.R., & Benjamins, V.R., (1998). Ontology of tasks and methods, knowledge acquisition workshop. *Banff*. http://ksi.cps.ucalgary.ca/KAW/KAW98/chandra/index.htm.

Crawford, C.S., Cully, A.C., Leutheuser, R., Sifuentes, M.S., White, L.H., & Wilber, J.P. (1993). Middle Rio Grande ecosystem: Bosque Biological Management Plan. The Middle Rio Grande Biological Interagency Team, US Fish and Wildlife Service, Albuquerque, NM.

Cleverly, J.R., Smith, S.D., Sala, A., & Devitt, D.A. (1997). Invasive capacity of Tamarix Ramosissima in a Mojavae Desert floodplain: the role of drought. *Oecologia*, 111:12-18

Dahm, C.N., Cleverly, J.R., Coonrod, J.E.A., Thibault, J.R., McDonnell, D.E., & Gilroy, D.J. (2002). Evapotranspiration at the land/water interface in a semi-arid drainage basin. *Freshwater Biology*, 47, 831-843

Frazier, P.S., & Kenneth, J. (2000). Water body detection and delineation with Landsat TM data. *American Society for Photogrammetry and Remote Sensing*, 55, 1461-1467

Frederico, F., Davis, C., & C?mara, G. (2003). Bridging ontologies and conceptual schemas in geographic information integration. GeoInformatica, 7, 344-378

Gamon, J.A., Field, C.B., Goulden, M.L., Griffin, K.L., Hartley, A.E., & Joel G., Penuelas, J., & Valentini, R. (2004). Relationships between NDVI, canopy structure, and photosynthesis in three Californian vegetation types. Ecological Application, 5, 28-41

Gao, B.-C. (1996). NDWI-A normalized difference water index for remote sensing of vegetation liquid water from space. *Remote Sensing of Environment*, 58, 257-266.

Gao, B.-C., & Goetz, F.H. (1995). Retrieval of equivalent water thickness and information related to biochemical components of vegetation canopies from AVIRIS data. *Remote Sensing of Environment*. 52, 155-162.

Horton, J.L., Kolv, R.W., & Hart, S.C. (2001). Responses of riparian trees to interannual variation in ground water depth in a semi-arid river basin. *Plant, Cell and Environment*, 24, 293-304

Howe, W.H., & Knopf, FL. (1991). On the imminent decline of Rio-Grande cottonwoods in central New Mexico. *The Southwestern Naturalist*, 36, 218-224

Innes, J.L., & Koch, B. (1998). Forest biodiversity and its assessment by remote sensing. *Global Ecology & Biogeography*, 7, 397-419

Katz, G.L., & Shafroth, P.B. (2003). Biology, ecology and management of *Elaeagnus Angustifolia L*. (Russian olive) in western North America. *The Society of Wetland Scientists*, 23, 763-777

Kokla, M., & Kavouras, M. (2001). Fusion of top-level and geographical domain ontologies based on context formation and complementarity. *International Journal of Geographical Information Science*, 15, 679-687

Lamberts, H., Chapin, F.S. III, & Pons, T.L. (1998). Plant Physiological Ecology. (pp. 5-6). New York: Springer

Langley, S.K., Cheshire, H.M., & Humes, K.S. (2001). A comparison of single date and multitemporal satellite image classification in a semi-arid grassland. *Journal of arid Environments*, 49, 401-411

Lillesaeter, O. (1982). Spectral reflectance of partly transmitting leaves: laboratory measurements and mathematical modeling. *Remote Sensing of Environment*, 12, 247-254

Maire, G. le, Francois, C., Dufrene, E. (2004). Towards universal broad leaf chlorophyll indices using PROSPECT simulated database and hyperspectral reflectance measurements. *Remote Sensing of Environment*, 89, 1-28

Martin, P.E. and Hagan RM. Evapotranspiration form riparian vegetation: Conserving water by reducing saltcedar transpiration. Journal of Soil and Water conservation. pp 237-239. July-August 1982.

McDonnell, D.E., Coonrod, J.A.E., & Dahm C.N. (2003). Changes in Vegetation along the Middle Rio Grande Riparian Corridor. International Symposium on Remote Sensing of Environment, Honolulu.

Mertes L. A. K. (2002) Remote sensing of riverine landscapes. *Freshwater Biology*. 47, 799-816.

Molles, M.C. Jr., Crawford, C.S., Ellis, L.M., Valett, H.M., & Dahm, C.N., (1998). Managed flooding for riparian ecosystem restoration. *BioScience*, 48, 749-756

Mouchot, M.C., Alfoldi, T., Delisle, D., & Mccullough, G., (1991). Monitoring the water bodies of the Mackenzie delta by remote-sensing methods. *Artic*, 44, 21-28

Nagler, P.L., Glenn, E.P., & Huete, A.R. (2001). Assessment of spectral vegetation indices for riparian vegetation in the Colorado river delta, Mexico. *Journal of Arid Environments*, 49, 91-110

National Resources Committee (1938). Regional Planning: Part VI- The Rio Grande joint investigation in the Upper Rio Grande basin in Colorado, New Mexico, and Texas (1936-1937), United States government Printing Office. For sale by the Superintendent of Documents, Washington, D.C.

Pearce, C.M., & Smith, D.G. (2001). Plains cottonwood's last stand: can it survive invasion of Russian olive onto the Milk River, Montana floodplain? *Environmental Management*, 28, 623-637

Ryherd, S., & Woodcock, C. (1996). Combining spectral and texture data in the segmentation of remotely sensed images. *Photogrammetric Engineering and Remote Sensing*, 62, 181-194

Sala, A., Smith, S.D., & Devitt, D.A. (1996). Water use by Tamarix Ramossissima and associated phreatophytes in a Mojave desert floodplain. *Ecological applications*, 6, 888-898

Shafroth, P.B., Auble, G.T., & Scott, M.L. (1994). Germination and Establishment of the Native Plains Cottonwood (*Populus deltoides* Marshall subsp. *monilifera*) and the Exotic Russian-olive (*Elaeagnus angustifolia* L.). Conservation Biology, 9, 1169-1175

Schultz, G.A., & Engman, E.T., (2000). Remote *Sensing in Hydrology and Water Management*. (pp. 11). New York: Springer

Sims, D.A., & Gamon, J.A. (2003). Estimation of vegetation water content and photosynthetic tissue area from spectral reflectance: a comparison of indices based on liquid water and chlorophyll absorption features. *Remote Sensing of Environment*, 84, 526-537

Smith, B., & Mark, D. (2001). Geographical categories: an ontological investigation. *International Journal of Geographical Information Science*, 15, 591-612

Spanner, M., Johnson, L., Miller, J., McDreight, R., Freemantle, J., & Runyou, P.G. (1994). Remote sensing of seasonal leaf area index across the Oregon transect. *Ecological Applications*, 4, 258-271

Stromberg, J.C. (1998). Functional equivalency of saltecedar *(Tamarix chinenis)* and Fremont cottonwood *(Populus fremontii)* along a free-flowing river. *Welands*, 18, 675-686

Taiz L and Zeigler Z. (1998) Plant Physiology 2nd edition. Sinauer Associates, Inc. Publishers. Sunderland, Massachusetts.

Tickner, D.P., Angold, P.G., Gurnell, A.M., & Mountford, J.O., (2001). Riparian plant invasions: hydrogeomorphological control and ecological impacts. *Progress in Physical Geography*, 25, 22-52

USGS Ground-water Resources of the Middle Rio Grande Basin, New Mexico, circular 1222. US Department of the Interior, US Geological Survey.

Welles, J.M. & Norman, J.M. (1991). Instrument for indirect measurement of canopy architecture. *Agron. J*., 83, 818-825.

Winter S. (2001) Ontology: buzzword or paradigm shift in GI science? *International Journal of Geographical Information Science*, 15, 587-590